ELSEVIER

Temperature prediction of rolling tires by computer simulation

Yeong-Jyh Lin, Sheng-Jye Hwang*

Department of Mechanical Engineering, National Cheng Kung University, Tainan, Taiwan

Abstract

A numerical procedure has been applied for investigating the temperature distribution in a smooth tread bias tire of a light truck, operated under different speeds, pneumatic pressures, and loading conditions. Prior to simulation by the finite element analysis, two separate sets of testing, namely dynamic mechanical testing and material testing, have been conducted in relation to the evaluation of hysteresis (H) and total strain energy (U_{sed}), respectively. Hysteresis loss energy is given as ($H \times U_{sed}$) and considered to relate directly to heat generation rate. Temperature rise is assumed to be due to the energy dissipation from periodic deformation. This dissipation of energy may be equated to be the primary heat generation source. Hysteresis energy loss is used as a bridge to link the strain energy density to the heat source in rolling tires; temperature distribution of rolling tires may be obtained by the steady-state thermal analysis. The above procedure has been shown to facilitate the simulation of the temperature distribution in the rolling tire.

An efficient computational process is being introduced to decrease the time for coupled 3D dynamic rolling simulation of tire. Temperature rise under different conditions is discussed with reference to the results of other published studies.
© 2004 IMACS. Published by Elsevier B.V. All rights reserved.

Keywords: 3D dynamic simulation; Rolling tires; Temperature distribution; Hysteresis loss

1. Introduction

Three decades have elapsed since the publication of a comprehensive monograph, providing an overall fundamental understanding of the mechanics of pneumatic tires [1]. Recently, high speed computational

* Corresponding author. Tel.: +886 6 2373144; fax: +886 6 2749411.
  E-mail addresses: n1889132@ccmail.ncku.edu.tw, jimppl@mail.ncku.edu.tw (S.-J. Hwang).

capability offered by software packages has aided the mathematical modeling and simulation in facilitating the analysis of the pertinent parameters. As such, through the popular use of the finite element analysis (FEA), significant results have been obtained for the modeling of the mechanics–material and structure–thermal properties of the rubber-based tires. In addition, the most publicized trend concerning the application of nanoscale science and technology to various human activities will include the design and manufacture of rubber-tires in response to improved performance; thus, a viable procedure of simulation in combination to actual testing will be needed for development undertaking by both tire manufacturers and users.

There have been substantial studies on the temperature distribution of tires for the purpose of technical performance and energy savings. However, considering the computational restriction, the temperature distributions have been determined by actual measurements on tires. To ease the necessity of the laborious testing, recent researchers have begun to analyze the related problems by computer simulation. Notably, Willett [2] used dynamic mechanical analyzer (DMA) to measure the properties of rubber material, and the temperature at the shoulder of tire was also measured at a fixed speed, loading, and inflation pressure.

Pillai and Fielding-Russell [3] used a load cell to measure the hysteresis ratio during loading and unloading process by fixing an experimental tire at a tension–compression tester. In their research, rolling
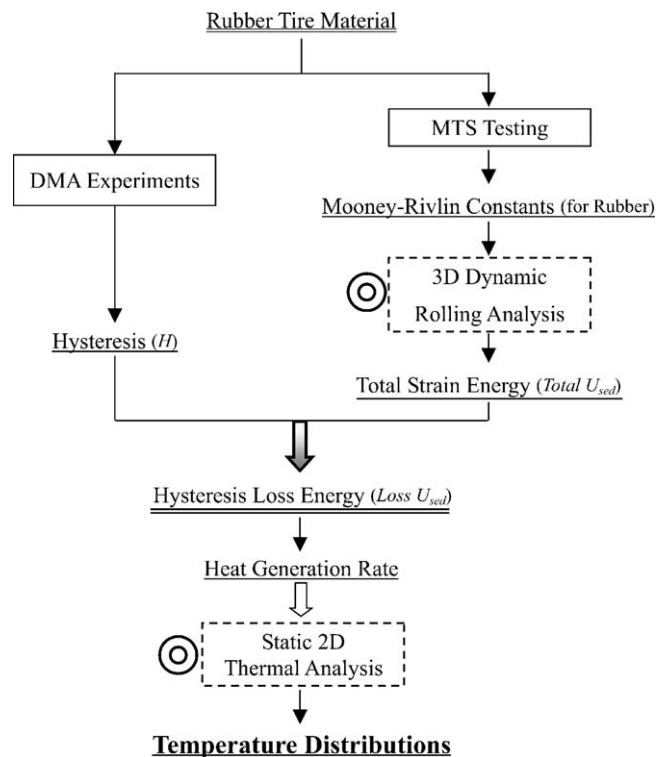

Fig. 1. A procedure for temperature distribution prediction with DMA experiment and finite element analysis (⊚ for the simulation analysis).

resistance was estimated by hysteresis ratio. Mc Allen et al. [4] predicted the inner and outer temperature distribution of aircraft tires by computer simulation. As a phase lag exists between the stress and strain, the hysteresis characteristic curve was derived by least square approximation with this material model. And then, the area inner the curve was taken as the loss energy for processing the temperature distribution of a tire. Ebbott et al. [5] derived the energy dissipation by combining computer simulation with visco-elastic material model. An equivalent elastic representation of the visco-elastic behavior is used in the FEA, providing the strain cycle to the energy dissipation module. However, effect of temperature and frequency on hysteretic energy loss was not considered in this study. Extensive future studies have been proposed.

The above brief literature search seems to indicate that further efforts are needed to correlate actual dynamic mechanical (DMA) testing and 3D temperature distributions by graphic depiction employing FEA for simulation. There have been substantial studies giving more or less reliable simulated results, based on a prior FEA, being validated by a subsequent actual testing. Also, there appears to be a consensus in that testing systems for both material testing and dynamic mechanical analysis are available, being easy to operate and control. Therefore, we have intended to approach the problem by first conducting separate mechanical and material testing; and then simulate the dynamics–temperature relationship in tires by FEA.

In the present study, computer simulation has been used to evaluate the temperature distribution of a smooth tread bias tire at different speeds, inflation pressure, and loadings. Our methodology employs two major sections as: dynamic rolling resistance simulation and heat transfer analysis; and the procedure is shown in Fig. 1. The heat generation rate has been obtained from the hysteresis energy losses. Total strain energy was obtained by dynamic rolling simulation of tire. Connecting with hysteresis data derived from a dynamic mechanical analyzer, hysteresis energy losses could be derived and used to predict the temperature distribution by steady-state thermal analysis.

2. Theoretical background

A brief review of the theoretical background for this study is given in the following, as:

2.1. Material properties

Rubber is the main element of tire, which can absorb the vibration and deformation for different loadings; it shows visco-elastic behavior that combines elastic and viscous characteristics. Cord ply networks are embedded in the rubber and preventing excessive deformation for rubber. The ring shape bead wire is the stiffening material in tire for constraining the deformation of both rubber and cord ply. During high speed driving, tires deform repeatedly and rapidly, and its visco elastic behavior leads to hysteresis. The temperature of a tire rises from the heat generation due to hysteresis effect, which is released from the kinematic deformation of the tire.

An overall discussion on the material characteristics has been given by Gehman [6] as: rubber structure and properties, friction of rubber, tire cord structure bonding and properties. Details may thus be relieved for simplicity.

2.2. Hysteresis

Hysteresis (*H*) is one of the most commonly used constants and defined as the energy loss part divided by the total energy in kinematic deformation cycle:

$$H = \frac{\text{Loss part}}{\text{Total part}} \tag{1}$$

Total part represents the total amount of input kinematic energy and the loss part represents the energy dissipated by the hysteresis effect. The loss energy is the main heat source for the temperature rise in a tire.

With DMA, the storage modulus (E') and loss modulus (E'') can be obtained. Then, the total input energy (E^*) can also be derived:

$$E^* = \sqrt{(E')^2 + (E'')^2} \tag{2}$$

Combining with Eq. (1), the hysteresis (*H*) could be estimated by Eq. (3) after DMA testing.

$$H = \frac{\text{Loss part}}{\text{Total part}} = \frac{E''}{E^*} \tag{3}$$

2.3. Total strain energy

The energy loss of a rolling tire was assumed coming from the deformation of rubber material in the tire. While deformation appears, the work done by external forces in producing deformation is stored within the body as the strain energy. And the strain energy per unit volume, dU/dV, is being referred as the strain energy density. Through the finite element simulation of a tire, one could obtain the strain energy density, which represents the total strain density of each deformed element. This strain energy density is defined as the total energy (Total U_{sed}) for the hysteresis in Eq. (1). The hysteresis in Eq. (1) is being rearranged as the loss strain energy density (Loss U_{sed}) over total strain energy density (Total U_{sed}), and represented in Eq. (4). Loss energy could be estimated if total energy and hysteresis (*H*) have been obtained.

$$H = \frac{\text{Loss part}}{\text{Total part}} = \frac{\text{Loss } U_{sed}}{\text{Total } U_{sed}} \tag{4}$$

2.4. Dissipative energy

By means of the DMA experiments of rubber and computer simulation of rolling tires, hysteresis (*H*) could be obtained. The total strain energy density (Total U_{sed}) was estimated by FEA simulation. Then, the loss strain energy density (Loss U_{sed}) per unit element could be estimated by multiplying hysteresis (*H*) by the total strain energy density (Total U_{sed}) via Eq. (4).

When calculating the total strain energy density from the rolling simulation, the strain and stress relation of each element rotating a cycle is obtained and is shown in Fig. 2. A second order polynomial curve may be sketched to fit the data; and the integrated area below the curve is reckoned as the dissipative energy for each axis-symmetric element. The dissipative strain energy is obtained via this way for each circumferential rubber elements.
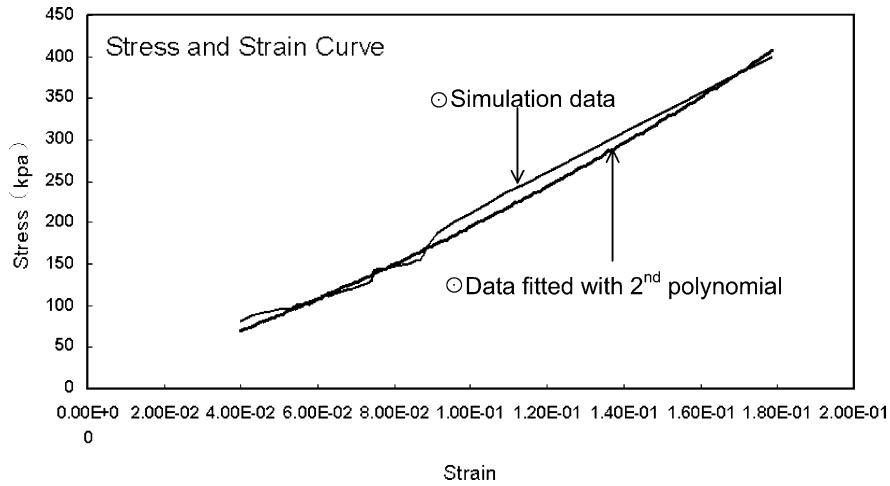
Fig. 2. Stress–strain relation of a rubber material element undergoing a circuit at the steady state from rolling simulation.

2.5. Heat generation rate

To predict the temperature distribution in a tire, the amount of dissipative energy should be estimated in the thermal analysis. Considering the rate of heat generated from hysteresis, the driving speed should be taken into consideration. Frequently rotation is represented by the number of cycles per second of the rolling tire and varies proportionally to the driving speed. Driving speed can be transferred into corresponding frequency (f):

$$f = \frac{V_c}{L_r} \tag{5}$$

$$L_r = 2\pi R_r \tag{6}$$

where V_c is the speed, L_r the circumferential length of the rolling tire, and R_r is the radius of rolling tire. The circumferential length of a rolling tire denotes the actual radius when the tire is running and it's deformed under thermal expansion, loading, and other factors. Then, the heat generation rate (H_G) was derived by the following equations.

$$H_G = \text{Loss } U_{sed} \times f = \frac{\text{Loss } U_{sed}}{\text{Unit Time}} \tag{7}$$

where f is the frequency and Unit Time denotes the time for the rolling tire complete one cycle. After the heat generation rate was obtained, the steady-state thermal analysis could be simulated with the basis of the proper heat convection and insulation boundary conditions, and thus the temperature distribution of a rolling tire at different conditions can be found.

2.6. Experiments

Two different experiments were performed to find the Mooney–Rivlin constants for dynamic rolling simulation and hysteresis for estimating the heat generation rate of rubber material.
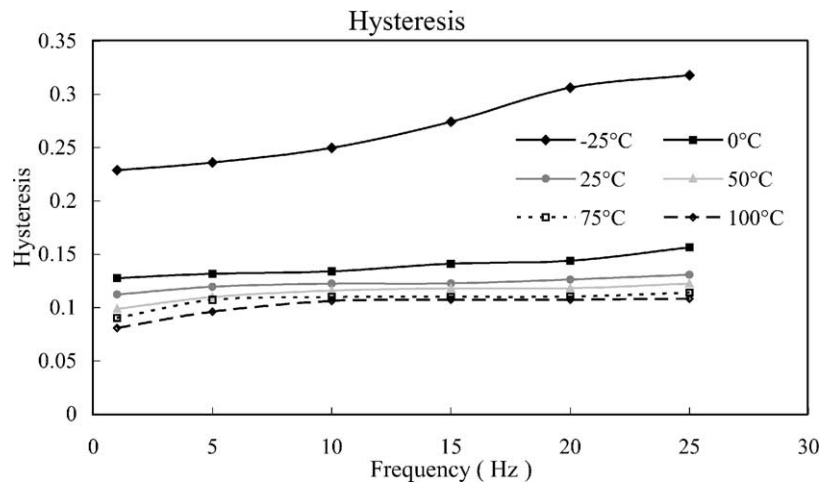
Fig. 3. Hysteresis for tread compound of bias tire varying with temperatures and frequencies.

2.6.1. Material testing system

By testing the specimen embedded with different angle cord ply, the elastic modulus was obtained by applying fiber-reinforced composite theory. And also the stress versus strain curve of the rubber material was obtained; and subsequently, the Mooney–Rivlin material model was used to obtain the Mooney–Rivlin constants.

2.6.2. Dynamic mechanical analyzer

The temperature varied continuously from -60 to $100\,^{\circ}$C during the DMA measurement. The hysteresis could be derived by Eqs. (2) and (3), which was shown in Fig. 3. As a tire is rolling, different speeds were transferred to the corresponding frequency by Eqs. (5) and (6). If the speed is 80 km/h, the frequency of the tire is 9.2 Hz. In this article, frequencies: 1, 5, 10, 15, 20, and 25 Hz were studied. This range of frequency represents a speed from 8.7 to 217.4 km/h.

From Fig. 3, hysteresis is noted to be almost of the similar values at different frequencies, especially when the temperature is above 25 °C. For this reason, the hysteresis (H) is assumed to be 0.1 for generating the hysteresis energy loss from total strain energy.

3. Simulation methodologies

For simplifying the problem, some reasonable assumptions and simplifications were made for the simulations:

1. Owing to the geometric symmetry, half of the tire is used in the simulation as shown in Fig. 4.
2. Assume that tires are consisted of rubber, cord plies, and steel wire.
3. Rubber is assumed to be isotropic, homogeneous, and fully cured in any part of the tire, and has hyper-elastic behavior through the entire temperature range.
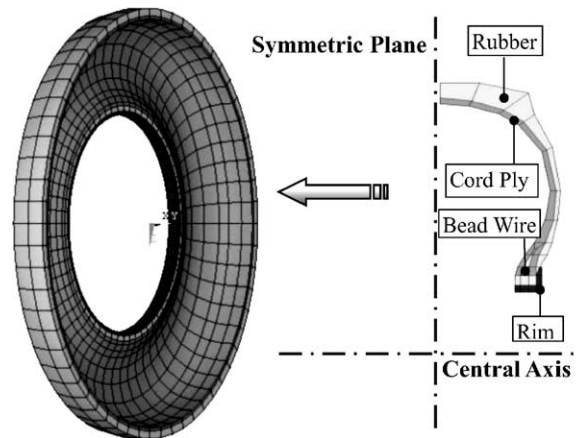
Fig. 4. Revolving 2D meshes with the central axis to form the 3D half FE model for rolling simulation and material distribution of tire in the cross-section view.

4. The cord ply and steel wire are elastic, isotropic, and homogeneous.
5. The road is assumed to be a rigid.
6. Neglecting the fluctuation of friction between the road and tire, and assume the friction coefficient between the road and tire is a constant: 0.1.

Half of the cross-section of the 3D model was constructed and shown in Fig. 4, which shown the material used in the tire for the simulation. The components in the tire were modeled by eight-node 3D elements. Material properties are summarized in Table 1. The mechanical and thermal properties of bead wire were taken as stainless steel. The thermal properties of rubber and cord ply specimens were provided by the manufacturer, and the mechanical properties such as elastic module, Poisson's ratio, and Mooney–Rivlin constants were obtained via the data derived from material testing.

Simulation methods are described in the following sequence: (1) dynamic rolling analysis and (2) steady-state thermal analysis. The software package employed for simulation work was that provided

Table 1
Material properties used in the simulation

Properties	Material		
	Rubber	Cord ply	Bead wire
Poisson's ratio[*]	0.49	0.3	0.3
Mass density (kg/m^3)[*]	1.2×10^3	1.1×10^3	6.5×10^3
Elastic modulus (Pa)[*]	–	500×10^6	207×10^9
Mooney–Rivlin constants[*]	$C_{10} = 0.1189 \times 10^6$, $C_{01} = -0.718 \times 10^5$	–	–
Thermal conductivity (W/m °C)[**]	0.293	0.293	60.5

[*] Obtained and calculated via the data derived from material testing experience.
[**] Provided by Kenda Rubber Industrial Corporation.

by ANSYS, Inc., as: Ansys/LS-Dyna for dynamic analysis and Ansys/Mechanical for thermal analysis [7].

3.1. Dynamic rolling analysis

As the real behavior of a rolling tire is in a transient state, it will take a long time for the computation to obtain the steady-state solution. In this section, an effective procedure was demonstrated to simulate the rolling condition at different speeds, inflation pressures, and loadings. The rolling analysis was separated into two steps:

3.1.1. Step 1: loading analysis
Different inflation pressures and loadings were simulated for obtaining the displacement without rolling, which was a static analysis. Steady-state results of displacements between road and tire under different conditions were obtained. Different loads (4, 6, 8 kN) were applied at the center of the tire, and inflation pressure (30, 50, 70 psi.) was applied at the inner surface. Boundary conditions were illustrated in Fig. 5. Loading effect was transferred to a displacement effect.

3.1.2. Step 2: rolling analysis
The displacement results from step 1 were set as the boundary conditions of upward displacement for road. To simulate the rolling effect, different speeds were applied to the road component, and friction coefficient was applied between the tire and road components to make the tire rolling. After the simulation, total strain energy density (Total U_{sed}) of the tire could be obtained. As this simulation was a dynamic analysis, it would take more computation resources than step 1.

Nine displacement results from step 1 and six different speeds (20, 40, 60, 80, 100, 120 km/h) were applied to the simulation. As a result, there were 54 cases simulated for study the
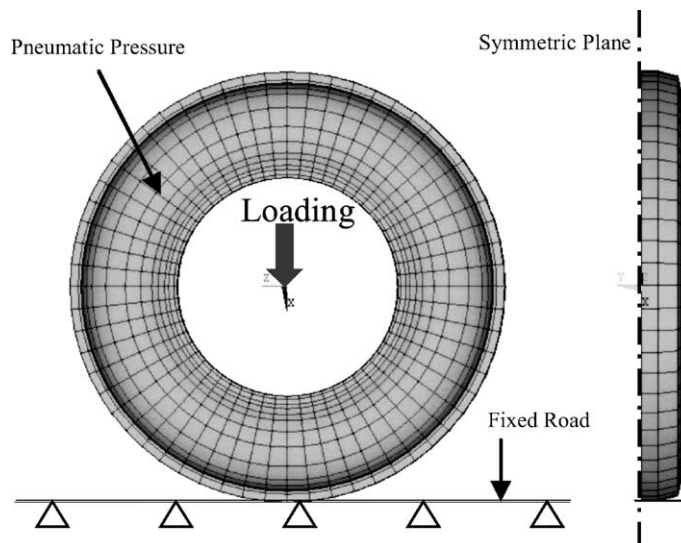

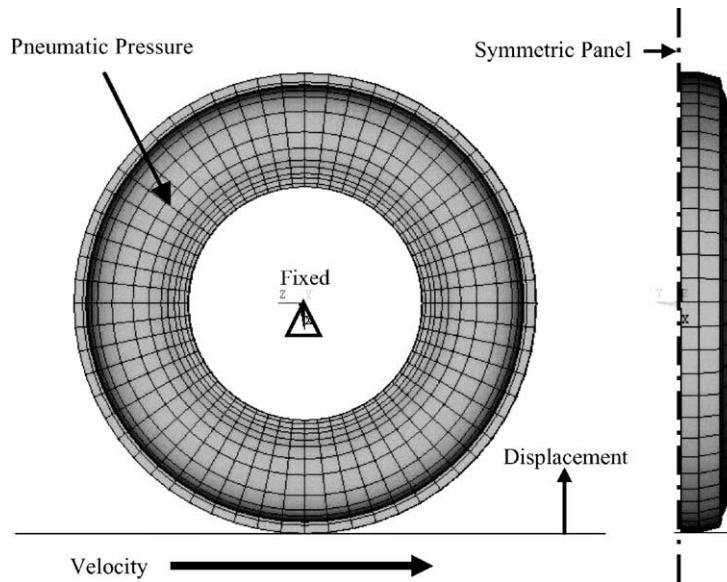Fig. 5. Boundary conditions for loading analysis.

Fig. 6. Boundary conditions for rolling analysis; upward displacement and velocity were applied to the road elements.

effect of different parameters. These boundary conditions applied to the model are shown in Fig. 6.

The approach used in step 2 was considered to be a displacement control. In reality, a tire has tended to deform by applying loads and is thus termed as, load control. The reason for using displacement control is to increase the convergence rate. If load control was used in the dynamic rolling analysis, not only damping ratio should be employed but also coupling loading and rolling analysis at the same time. Therefore, it would take longer time to obtain the steady-state dynamic solution. Although the displacement control procedure does not generate "true" dynamic simulation results, but these results are sufficient for current application and the amount of computer resources needed for the simulation is greatly reduced.

3.2. Steady-state thermal analysis

From Eq. (1), the term "Loss part" is the main cause of temperature rise in a tire, which can be considered as the dissipative energy. From the DMA experiment, hysteresis was derived and approximated to be 0.1, and total strain energy density could be found from rolling simulation. By Eq. (4), the Loss U_{sed} was derived, and then the heat generation rate (H_G) could also be obtained by Eq. (7) for each rubber elements.

When the temperature of a tire is coming to the steady state, the temperature distribution is a 2D axis-symmetric distribution. As a result, half of the axis-symmetric 2D FEM model, being considered as equivalent to the 3D rolling simulation model, and is shown in Fig. 7.

Heat generation rate (H_G) was applied for each rubber element as the major heat source, and forced convection coefficient was applied at the outer surface by $5.9 + 3.7 v$ W/m^2 °C (v is the air speed in m/s) [5]. Schematic of the boundary conditions was shown in Fig. 7. Thermal conductivity of the materials were shown in Table 1.
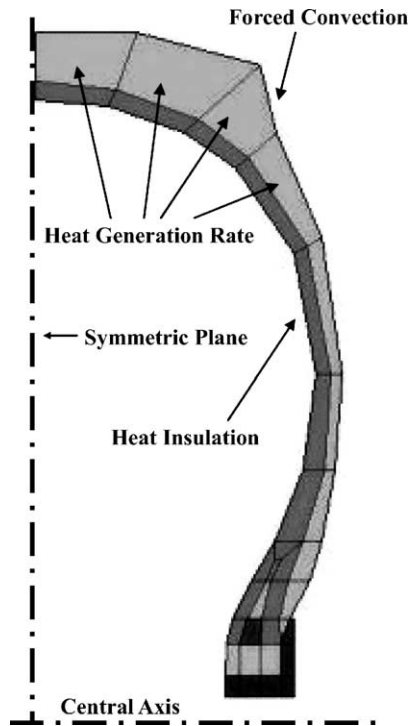
Fig. 7. Boundary conditions for the 2D thermal analysis. (Inner surface was insulated and outer surface was applied with forced convective condition.)

4. Results and discussions

4.1. Loading analysis

Data of loading experiments, performed by the laboratory of Kenda Rubber Industrial Corporation, have been used to verify the simulation result. Displacement results under different loadings and inflation
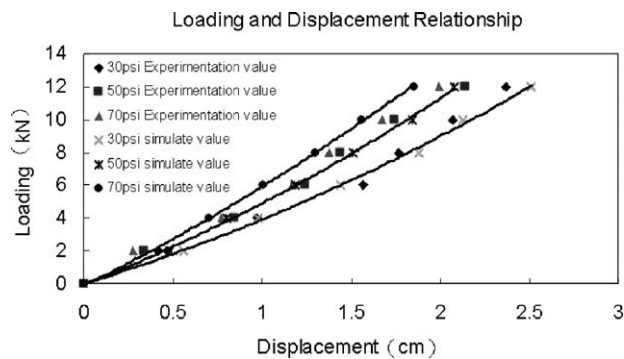

Fig. 8. Comparison of the simulated and experimental tire loading results, the solid lines was fitted with second polynomial by simulation results.
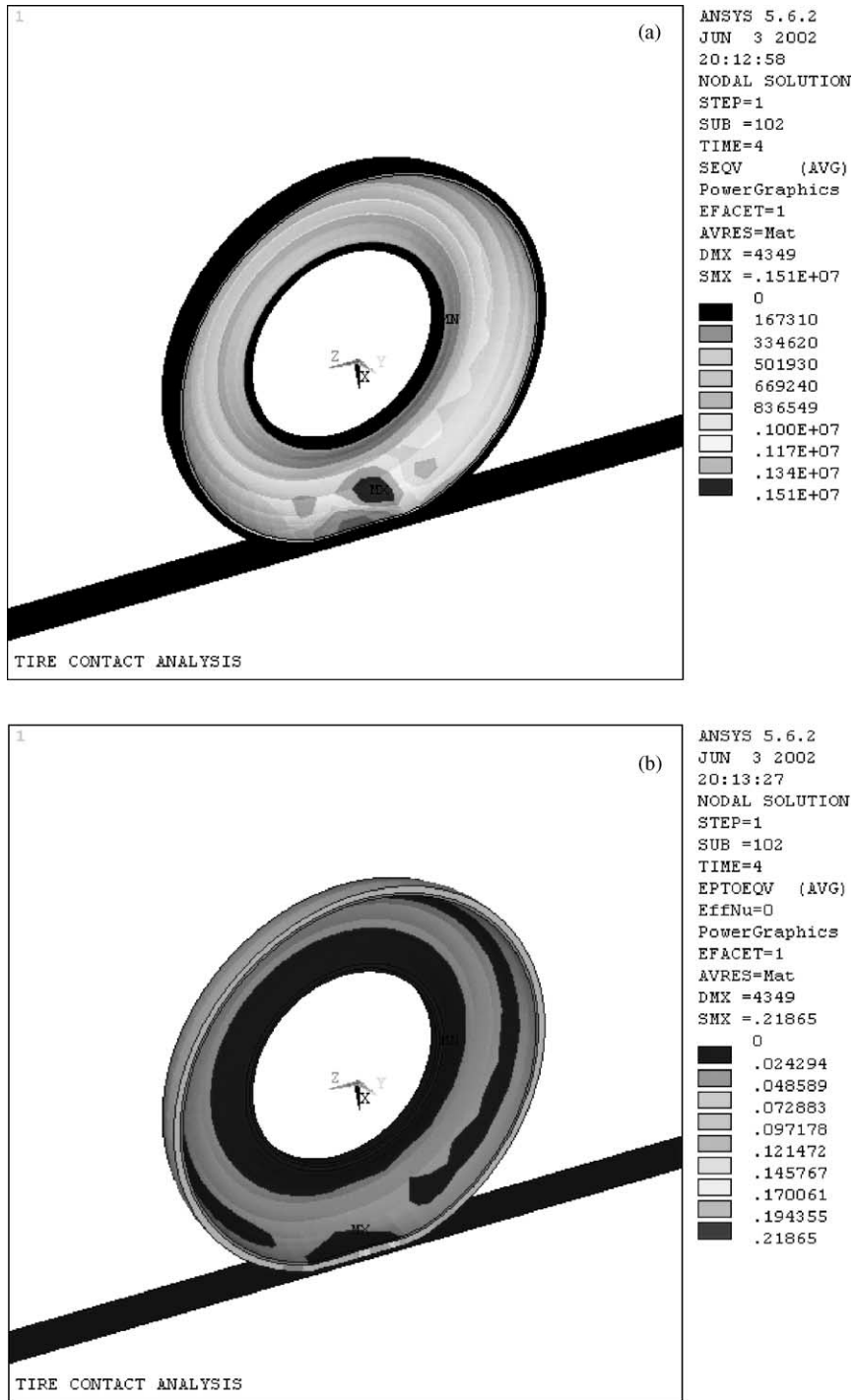
Fig. 9. (a) Equivalent stress distribution of a rolling tire, under the pneumatic pressure of 70 psi, loading of 6 kN, and velocity of 100 km/h (unit: g/cm s^2). (b) Equivalent strain distribution of a rolling tire, under the pneumatic pressure of 70 psi, loading of 6 kN, and velocity of 100 km/h.

pressures were obtained by experiments. The experiment and simulation results of displacement are compared in Fig. 8. From Fig. 8, each solid line is the second order polynomial curve fitting by the simulation data of three different pressures, and one could find that the experiment and simulation results have the same trend and the agreement seems to be adequate.

4.2. Rolling analysis

In each rolling analysis, numerous data would be obtained, such as stress, strain, deformation, strain energy, principal stress, and so on. The non-axial symmetric distribution of equivalent stress and equivalent strain are shown in Fig. 9(a) and (b) (condition: 70 psi–6 kN–100 km/h). The distribution of the equivalent stress and strain for other cases with different loading, inflation and speed conditions are substantially similar to the results as shown in Fig. 9(a) and (b).

4.3. Thermal analysis

Through the steady-state thermal analysis, the temperature distribution of different cases can be found. Taking the case with inflation pressure–load–speed 70 psi–4 kN–20 km/h as an example, thus temperature distribution is shown in Fig. 10. It may be note that the maximum temperature occurs at the shoulder of the tire.
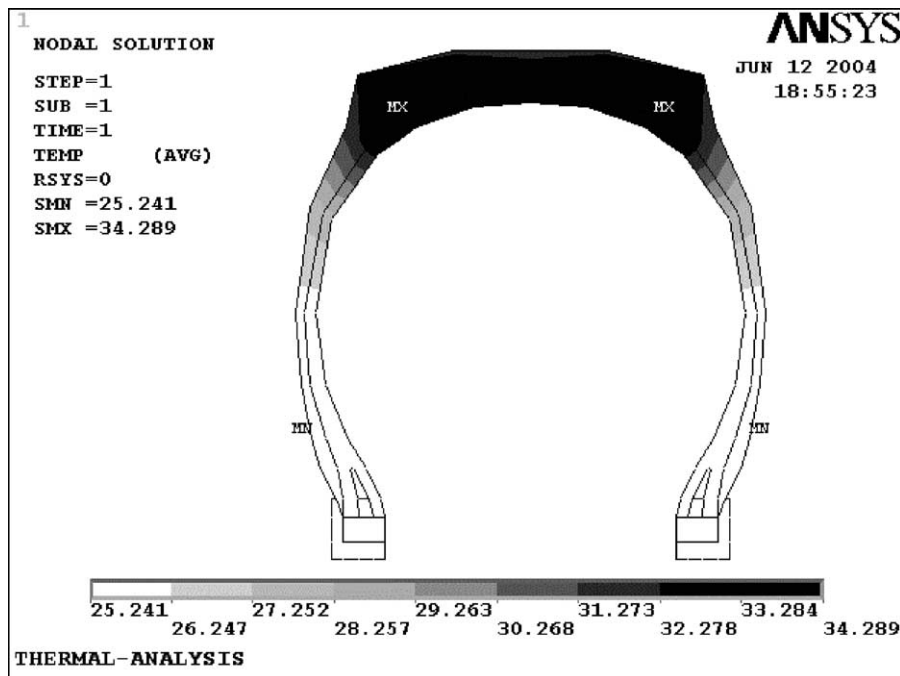

Fig. 10. Two-dimensional temperature distribution of a tire under 70 psi–4 kN–20 km/h, and maximum temperature occurring at the shoulder (unit: °C).
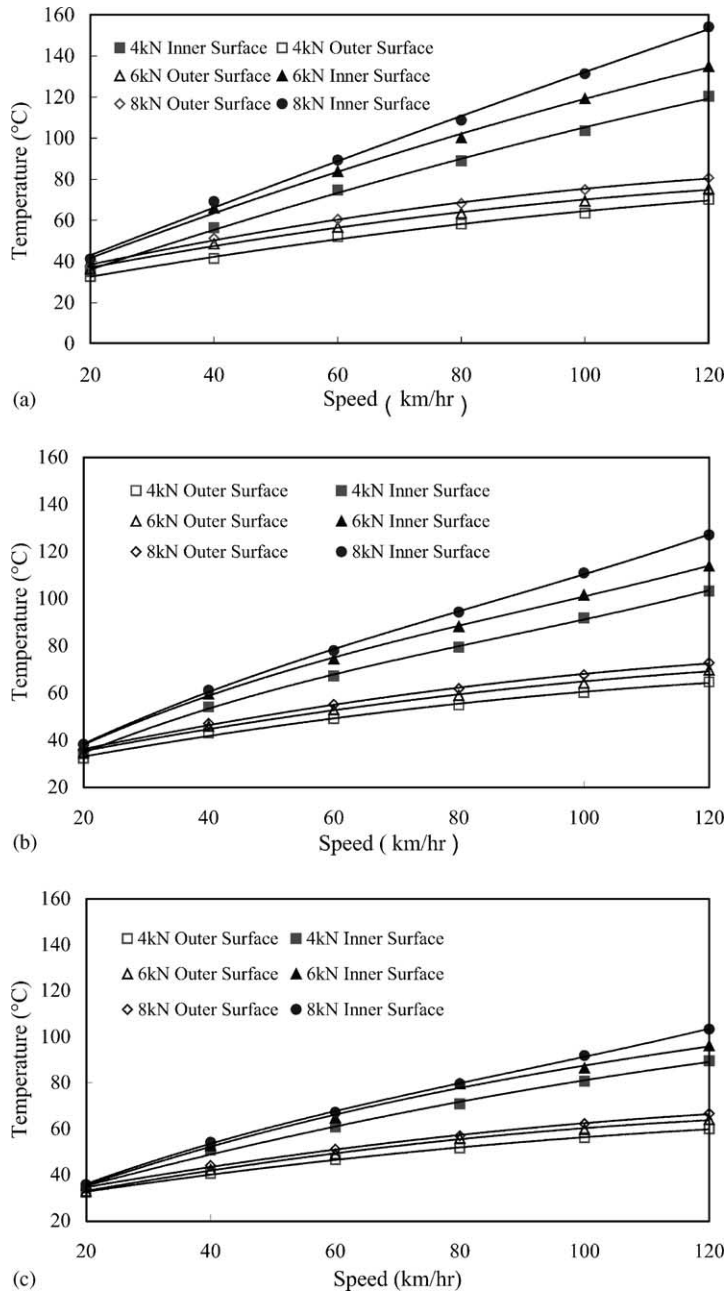
Fig. 11. (a) Temperature at shoulder under an inflation pressure of 30 psi (maximum temperature, 154 °C). (b) Temperature at shoulder under an inflation pressure of 50 psi (maximum temperature, 127 °C). (c) Temperature at shoulder under an inflation pressure of 70 psi (maximum temperature, 103 °C).
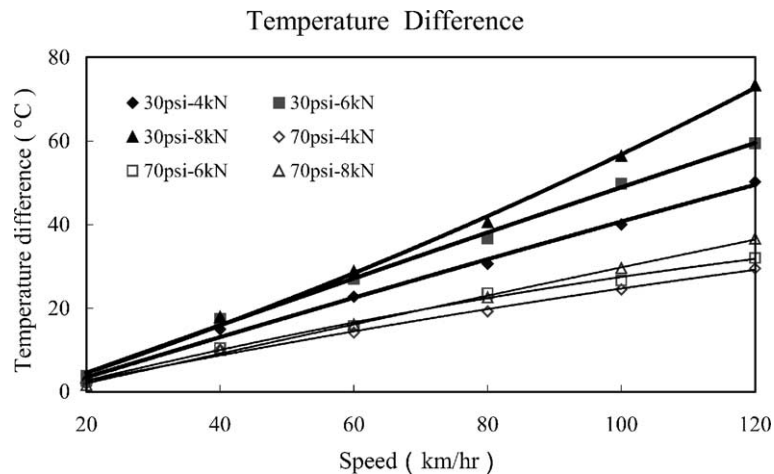
Fig. 12. Temperature difference of inner and outer surface.

Thus, the thermal analysis has been shown to be capable for giving the temperatures at different locations of the tire. The maximum temperatures of tire with difference inflation pressures are shown in Fig. 11(a–c). From these figures, it may be found that the inner surface temperature is higher than that of the outer surface since there is convection on the outer surface. Besides, it is also shown that the temperature increase is due to the effects of increasing both speed and loading or decreasing tire inflation pressure. The inflation pressure seems to have more influence on temperature rise than that of loading.

The temperature differences, between the inner and outer surfaces of the tire are shown in Fig. 12, and it was found that increasing the inflation pressure would reduce the temperature difference between the inner and outer surfaces at the shoulder. The above results are noted to be more or less similar to that of pneumatic aircraft tire computed via FEM by Mc Allen et al. [4].

5. Conclusion

A numerical procedure is proposed in this paper to predict the temperature distribution of a rolling tire of a light truck. This evaluation system sequentially combines both MTS and DMA experiments with computer simulation, and is found to be effective. Computational resource is greatly reduced for separating the dynamic rolling analysis into static loading analysis and rolling analysis.

From this investigation, the following conclusions can be drawn:

1. Hysteresis effect has been noted to increase for the increasing loading and decreasing inflation pressure; thus, the lead temperature difference between the inner and outer surface becomes more obviously.
2. The amount of energy that is being transferred from hysteresis energy loss to heat increases with increasing rolling speed, seems to be responsible for the temperature rises at the inner surface more quickly, especially at the shoulder.
3. It has been found that inflation pressure plays an important role for the temperature rise of a rolling tire. Increasing the pressure will reduce the hysteresis effect, and decrease the temperature at the shoulder.

Acknowledgements

References

[1] S.K. Clark, Mechanics of Pneumatic Tires, Office of Vehicle Systems Research, Institute for Applied Technology and National Bureau of Standards, Washington, 1971, pp. 596–597.

[2] P.R. Willett, Hysteretic losses in rolling tires, Rubber Chem. Technol. 46 (1973) 425–441.

[3] P.S. Pillai, G.S. Fielding-Russell, Tire rolling resistance from whole-tire hysteresis ratio, Rubber Chem. Technol. 65 (1992) 444–452.

[4] J. Mc Allen, A.M. Cuitino, V. Sernas, Numerical investigation of the deformation characteristics and heat generation in pneumatic aircraft tires, Finite Elem. Anal. Design 23 (1996) 241–290.

[5] T.G. Ebbott, R.L. Hohman, J.-P. Jeusette, V. Kerchman, Tire temperature and rolling resistance prediction with finite element analysis, Tire Sci. Technol. 27 (1999) 2–21.

[6] S.D. Gehman, Material characteristics in mechanics of pneumatic tires, in: S.K. Clark (Ed.), Mechanics of Pneumatic Tires, Office of Vehicle Systems Research, Institute for Applied Technology and National Bureau of Standards, US Department of Commerce, Washington, 1971, pp. 1–40.

[7] Anon, ANSYS Theory Manual, Release 5.7, 2001.